Lab on a Chip

COMMUNICATION

View Article Online
View Journal | View Issue

Check for updates

Cite this: *Lab Chip*, 2019, **19**, 2156

Received 16th May 2019,
Accepted 27th May 2019

DOI: 10.1039/c9lc00460b

rsc.li/loc

Published on 28 May 2019. Downloaded by York University on 6/25/2019 5:11:38 PM.

Non-aqueous continuous-flow electrophoresis (NACFE): potential separation complement for continuous-flow organic synthesis†

Nikita A. Ivanov, Yimo Liu, Sven Kochmann and Sergey N. Krylov *

We introduce non-aqueous continuous-flow electrophoresis (NACFE) in which the electrolyte is a solution of an organic salt in an aprotic organic solvent. NACFE can maintain steady-state separation of multiple hydrophobic organic species into individual molecular streams. It is a potential separation complement for continuous-flow organic synthesis. This proof-of-concept work will serve as a justification for efforts towards making NACFE a practical tool in flow chemistry.

Continuous-flow organic synthesis has a number of important advantages over its batch counterpart.[1–4] Continuous-flow separation of multiple components of the reaction stream (*e.g.* products, intermediates, excess reactants, catalysts, *etc.*) from each other is often required between the stages of continuous-flow organic synthesis.[5] Liquid–liquid extraction that segregates molecules through their partitioning between organic and aqueous phases is the most common continuous-flow separation method.[6,7] Yet, it can hardly separate hydrophobic organic molecules with similar partition coefficients from each other.[8] Continuous-flow electrophoresis (CFE), which is also called free-flow electrophoresis, can support much more selective separation.[9–11] Its ability to separate multiple molecular streams in a single phase could potentially facilitate its seamless integration with continuous-flow organic synthesis. However, practical CFE has been so far limited to aqueous electrolytes; with an exception of a single work by Bowser and co-authors reporting the use of a non-aqueous electrolyte including a protic organic solvent (methanol).[12] Aqueous electrolytes are incompatible with continuous-flow organic synthesis, as the synthesis often involves reaction components insoluble in water or sensitive to aqueous media.[13] An additional problem with aqueous electrolytes is intensive gas formation during water electrolysis; hardly avoidable accumulation of gas bubbles in the separation chamber makes steady-state operation of CFE a technical challenge (protic organic solvents suffer from the same problem).[14–16] On the contrary, non-aqueous continuous-flow electrophoresis (NACFE) could potentially use aprotic organic solvents which are not only compatible with solvents utilized in continuous-flow organic synthesis but also could reduce gas formation and make separation stable without elaborate technical solutions. Owing to these two anticipated advantages, NACFE utilizing aprotic organic solvents appears to be a highly attractive separation complement for continuous-flow organic synthesis (Fig. 1a). Devices for NACFE are simple and can be easily custom fabricated (Fig. 1b). Therefore, it is rather surprizing that there have been no reports on this technique while aprotic non-aqueous electrolytes, *e.g.* based on cyclic carbonates, are widely used in batteries,[17] and have been used in discontinuous separation by capillary electrophoresis.[18] The goal of this work was to prove the feasibility of NACFE with aprotic electrolytes and test its suitability for steady-state separation of multiple molecular streams in organic phase.

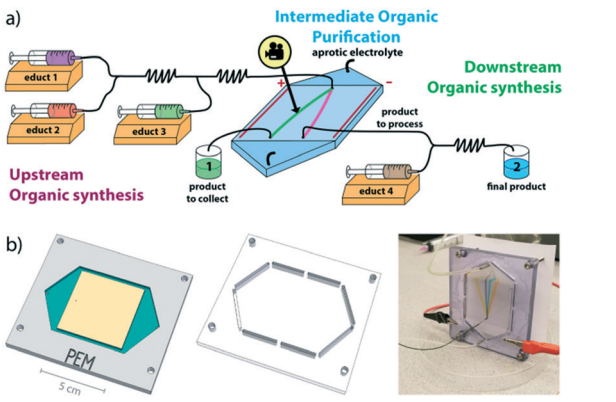

Fig. 1 a) Schematic of NACFE seamlessly integrated between two stages (upstream and downstream) of continuous-flow organic synthesis. b) Geometry of the bottom part (left) and top part (middle) of the NACFE chip used in this study as well as its photo in operation (right).

Centre for Research on Biomolecular Interactions and Department of Chemistry, York University, Toronto, Ontario M3J 1P3, Canada. E-mail: skrylov@yorku.ca

† Electronic supplementary information (ESI) available. See DOI: 10.1039/c9lc00460b

This journal is © The Royal Society of Chemistry 2019

Published on 28 May 2019. Downloaded by York University on 6/25/2019 5:11:38 PM.

Continuous-flow separation (as an integral part of continuous-flow synthesis) must operate under steady-state conditions. We, thus, aimed at developing steady-state NACFE confirmed by stable uninterrupted operation during *e.g.* a 10 h shift. Separation instability in CFE is caused by gradually growing distortion of the hydrodynamic flow and/or electric field during the course of operation. The major and very persistent cause of such distortion is the hardly-avoidable accumulation of gas bubbles in the device.[14–16] The most straightforward long-term solution for this problem is bubble evacuation to the atmosphere through an open-electrolyte approach.[14] This approach should, however, be avoided for non-aqueous electrolytes due to safety concerns. Thus, we limited ourselves to closed NACFE devices. In NACFE, one can foresee another potential source of growing distortion of hydrodynamic flow: deterioration of the electrophoretic device under the influence of an organic solvent. Hence, a NACFE device must be made of a solvent-resistant material. We chose propylene carbonate (PC) as an aprotic organic solvent, and had to use a device material resistant to it. While silica glass is arguably the best choice of a solvent-resistant optically-transparent material, making prototype NACFE devices of HF-etched glass is not as practical as making them of mechanically-machined plastics. We tested a set of 18 plastics, commercially available in sheets, for their machinability, optical clarity, and resistance to PC (Table S1, ESI†). Three of them, fluorinated ethylene propylene, polyvinyl chloride (PVC) type I, and polysulfone, were found potentially suitable based on these three parameters. Of these three plastics, we chose PVC type I for its optical clarity, cost efficiency, and full suitability for device-fabrication procedures previously developed for poly(methyl methacrylate).[19,20] A NACFE chip of a basic geometry (Fig. 1b and S1, ESI†) was fabricated and used for all experiments described below.

A key component of any electrolyte is a charge carrier, which is typically a well-soluble non-reactive salt giving a free cation and a free anion upon dissociation. Two types of organic salts have been previously used as charge carriers in non-aqueous aprotic electrolytes in capillary electrophoresis: tetraalkylammonium salts and imidazolium salts (ionic liquids).[21,22] Their use in capillary electrophoresis did not guarantee transferability to NACFE for two reasons. In contrast to capillary electrophoresis, electrodes in NACFE are inside the separation chamber making NACFE susceptible to instability associated with electrochemistry of electrolyte components. In addition, capillary electrophoresis runs take only a few minutes, and long-term stability is not a requirement in contrast to NACFE. Therefore, we first tested NACFE for long-term stability of electric current and optical properties of the chip. The experiment was done for two electrolytes: solutions of tetrabutylammonium acetate (TBAA) and imidazolium ethyl sulfate in PC. We found that the electrical current was stable for TBAA during a 10 h run (Fig. S2, ESI†). No gas bubble accumulation was evident. Minor precipitation could be noticed at the cathode side of the NACFE chip likely due to an electrochemical reaction involving tetrabutylammonium. This precipitate did not affect the optical clarity of the chip. In contrast, we found the excessive formation of a brown precipitate at the cathode side of the chip for the imidazolium electrolyte (Fig. S3, ESI†). The precipitate was most likely an insoluble product of an electrochemical reaction involving imidazolium.[23] This precipitate affected the optical clarity of the chip and could interfere with optical detection; accordingly, we ruled out imidazolium-based electrolytes from our further consideration. Hence, a solution of TBAA in PC was chosen as a default electrolyte for the rest of this NACFE study.

Next, we tested separation of multiple molecular streams in NACFE (Fig. 2). As molecules to be separated we used 2-4-(dimethylamino)styryl-1-methylpyridinium (DMAS), Sudan black B, α-naphtholbenzein, and fluorescein (the first three are hydrophobic and poorly soluble in water). All of them are chromophores visible to the naked eye, which facilitated easy detection of their streams in this proof-of-feasibility work.

The quality of NACFE was assessed using a recently introduced approach based on angulagram representation of molecular stream separation and four quantitative characteristics: stream deflection, stream width, stream linearity, and resolution of two streams.[24] Images of molecular streams in NACFE were recorded with a consumer photo camera. These images were processed automatically to construct angulagrams and compute the quantitative characteristics of the streams (see ESI† for details on these procedures and corresponding custom-designed software).

All molecular streams shown in Fig. 2 were deflected as predicted by the previously proposed separation mechanism based on heteroconjugation.[25,26] Briefly, small anions (*e.g.* acetate) form heteroconjugates with hydrogen-bond donors. The effective charge of a heteroconjugate is negative and its

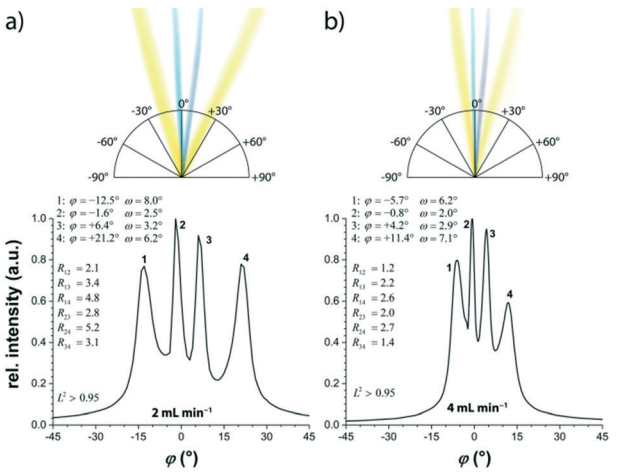

Fig. 2 Angulagrams of NACFE of fluorescein,[1] α-naphtholbenzein,[2] Sudan black B,[3] and DMAS[4] (1.25 mM each) in 30 mM TBAA in PC at two different electrolyte flowrates: a) 2 and b) 4 mL min^{-1}. The values in the graph are stream deflection (φ), stream width (ω), stream linearity (L^2), and resolution of stream n from stream m (R_{nm}). NACFE was run with E = 27.3 V cm^{-1} (I = 8.3 mA) and a sample flowrate of 2 μL min^{-1}. The anode and cathode are towards negative and positive angles, respectively.

Published on 28 May 2019. Downloaded by York University on 6/25/2019 5:11:38 PM.

magnitude depends on the degree of heteroconjugation; this dependency is advantageous as it allows, for instance, the separation of different phenols. In our case, α-naphtholbenzein (phenol) and fluorescein (carboxylic acid and phenol) formed negatively charged heteroconjugates, which were deflected towards the anode. DMAS is not a hydrogen-bond donor but possesses one quaternary nitrogen atom with a positive charge. Hence, DMAS was deflected towards the cathode. Sudan black B has no positive charge and is assumed to be a very weak hydrogen-bond donor, which, however, still can experience a low degree of heteroconjugation. Therefore, its stream was expected to be deflected slightly towards the anode, *i.e.* negative angles in the angulagram in Fig. 2. In fact, it was deflected towards the cathode, *i.e.* positive angles. This small deflection was due to the presence of the electroosmotic flow[27–29] (from anode to cathode) and affected deflection of other streams as well. Ideally, one would compare the experimental deflection angles to theoretical ones;[24] however, the theory for calculating electrophoretic mobilities (which define deflection angles) is not straightforwardly applicable to non-aqueous electrophoresis. All streams in Fig. 2 are linear ($L^2 > 0.95$) and narrow (<10° in width). The worst stream resolution ($R > 1.2$) in Fig. 2 is still sufficient for collecting any individual stream with hardly any overlap with any other stream ($R \geq 1.0$ is our threshold for collectable streams[24]); in the particular case in Fig. 2b, α-naphtholbenzein and Sudan black B can be collected with ≈98% purity assuming normal distributed stream profiles at the end of the chip. Increasing the concentration of the charge carrier in the electrolyte expectedly led to improved separation confirmed by decreasing stream width and increasing linearity (Fig. 3).

Unsurprisingly, no separation could be observed when the electrolyte was replaced with pure PC without any charge carrier. Adding a charge carrier at a concentration (3.3 mM) similar to the analyte concentrations (1.67 mM) resulted in one broad stream (width: 9.8°) in which the individual analytes started to separate. Increasing the charge carrier concentration from 3.3 to 10 mM (an order of magnitude higher than the analyte concentrations) turned this broad stream into individual narrow ones (widths of 4.4 to 6.8°); further increase to 30 mM narrowed the streams even more (widths of 2.3 to 4.5°). The carrier concentration had only minimal effect on the linearity; linearity increased from 0.90 to 1.00 with carrier concentration increasing from 0 to 30 mM. Increase in the carrier concentration progressively suppresses the electroosmotic flow directed towards the cathode.[30] Hence, stream deflections changed towards the anode with increasing carrier concentration. For instance, the stream deflection of Sudan black B changed from +13.4 to +3.0° (*i.e.* became less deflected) when the carrier concentration was increased from 0 to 30 mM. Increasing the carrier concentration above 100 mM, *e.g.* for increasing the concentrations of separated species, will be associated with increased Joule heating and worsening quality of separation.

The quality of separation depended on the nature of the anion in the charge carrier. A weak-base anion (*e.g.* hydrogen sulfate) could not support the separation of α-naphtholbenzein from Sudan black B, while a strong base (*e.g.* acetate) could separate them (Fig. S4, ESI†). All results discussed above are consistent with the aforementioned separation mechanism in NACFE, in which heteroconjugation of electrolyte anions with hydrogen-bond donors plays a key role (see above).[25,26]

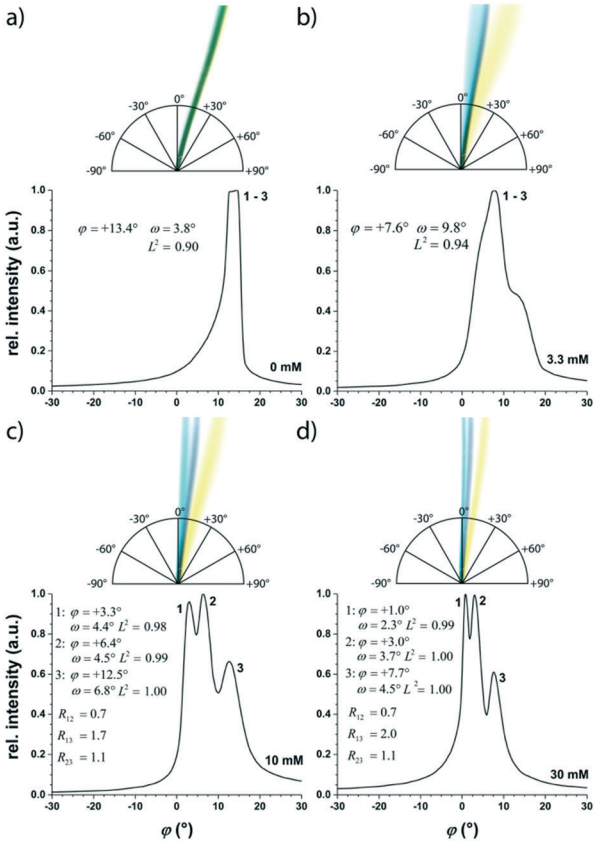

Fig. 3 Angulagrams of NACFE of α-naphtholbenzein,[1] Sudan black B,[2] and DMAS[3] (1.67 mM each) under various concentrations of TBAA in PC: a) 0, b) 3.3, c) 10 and d) 30 mM. Given are stream deflection (φ), stream width (ω), stream linearity (L^2), and resolution of stream n from stream m (R_{nm}). E = 27.3 V cm^{-1} was used in all experiments and resulted in currents of 0.07 (a), 1.26 (b), 3.69 (c), and 9.9 mA (d). The flowrates were 3 mL min^{-1} for the electrolyte and 2 μL min^{-1} for the sample. The anode and cathode are towards negative and positive angles, respectively.

Finally, we examined whether steady-state NACFE could be maintained (*e.g.* stable separation during a 10 h shift), which is the key requirement for integrating NACFE with continuous-flow synthesis. Three hydrophobic analytes were used in this experiment: α-naphtholbenzein, Sudan black B, and DMAS. The electrolyte was recycled roughly every 2.5 h to minimize material waste; we did not interrupt separation for electrolyte recycling. Our results show no significant deterioration in stream deflection, width or linearity during the 10 h NACFE with the exception of stream width for α-naphtholbenzein which drifted from 5 to 12° (Fig. 4). This degree of stream widening, however, would not affect

 This journal is © The Royal Society of Chemistry 2019

Published on 28 May 2019. Downloaded by York University on 6/25/2019 5:11:38 PM.

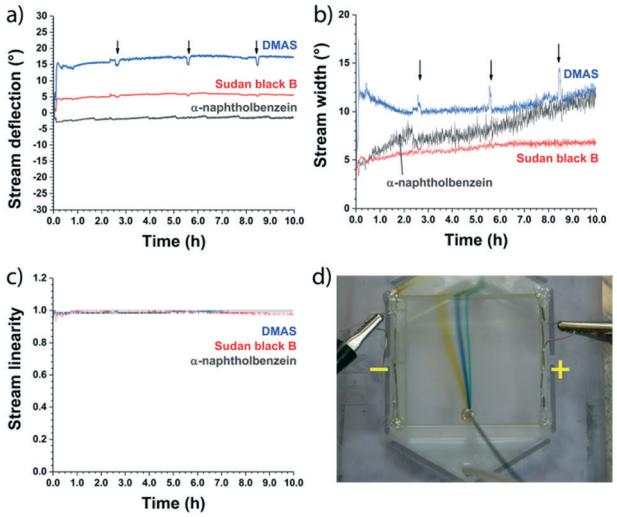

Fig. 4 a–c) Stream parameters and d) an averaged photo (3587 images were integrated for visual assessment of separation stability) of 10 h NACFE of α-naphtholbenzein, Sudan black B, and DMAS (1.67 mM each) in 30 mM TBAA in PC. Recycling was done roughly every 2.5 h (marked with arrows).

significantly stream collection for the observed magnitudes of resolution and stability of deflection.

In the frame of the present work, we also explored the option of using acetonitrile instead of PC in NACFE. Our results demonstrate that separation in acetonitrile-based electrolytes is possible in principle (Fig. S5, ESI†). However, electrolytes based on PC beneficially allowed lower flowrates (due to lesser gas bubble formation) and higher electric fields (due to lower currents and Joule heating). Furthermore, PC is a less toxic, less volatile, and more viscous solvent than acetonitrile.[31,32] Thus, we did not further investigate acetonitrile in the frame of this work. However, the interested reader is referred to an excellent work by the Belder group that was published after the original submission of our manuscript and which completely focuses on acetonitrile as a solvent in NACFE.[33]

Finally, we would like to address the issue of obtaining a pure product after the separation by NACFE using our specific case as an example. The solvent outflow collected at the terminal end of the separation zone contains a product mixed with an excess of electrolyte. Both the electrolyte (TBAA) and the solvent (PC) need to be removed to yield a pure product. Based on our practical experience with PC (ESI†), we see three options to achieve this goal. The first option is a liquid–liquid extraction of the electrolyte from propylene carbonate with an equal volume (50 : 50 v/v) of water, followed by vacuum assisted rotary evaporation of the remaining propylene carbonate. The second alternative is to precipitate a product from the PC–TBAA mixture with an excess of water (higher than 4 : 1 volume ratio). The precipitated product can then be filtered and washed with cold water to remove all remaining TBAA. The third option is a liquid–liquid extraction of the product directly from PC using hexane or the like. For this, of course, the product has to be soluble in hexane. Hexane can then be removed by vacuum assisted rotary evaporation. Obviously, the choice of most suitable option depends on the properties of the product to be separated and purified. Furthermore, the in-flow implementation is not as straightforward and requires some engineering.

In conclusion, we proved the feasibility of NACFE with an aprotic electrolyte, namely TBAA in PC, by demonstrating steady-state separations of multiple molecular streams. This proven feasibility should stimulate efforts to implement integrated NACFE/continuous-flow synthesis. Here, we would like to outline what is required for such an implementation. First, any NACFE device must have outputs for multiple molecular streams; such devices have been successfully fabricated and used in the past.[34–36] Second, the optimization of device operation, *e.g.* adjustment of electric field and flowrate, requires visualization/detection of separated molecular streams. Most organic molecules are not chromophores visible to the naked eye but absorb UV light; therefore, UV-imaging of a large area of the NACFE chip is required. Belder and co-authors have recently demonstrated deep-UV fluorescence imaging of UV-absorbing molecular streams in a small CFE chip.[37,38] This is a promising approach towards UV-imaging of larger chips. However, significant increases in scanning speed and covered area are required to apply this approach to real-time imaging of larger chips. We foresee that solving this challenging detection issue will open the way for practical use of NACFE in combination with continuous-flow synthesis. It is important to emphasize that In contrast to liquid–liquid extraction, which has no intrinsic detection capability and requires secondary analysis, *e.g.* by HPLC, CFE has a unique capability of real-time quantitative detection, which makes such secondary analyses unnecessary.

This work was supported by a grant from Natural Sciences and Engineering Research Council of Canada to SNK (grant number STPG-P 521331-2018). The authors thank Dr. Boris Gorin (Senior Scientific Advisor, Alphora Research Inc.) for valuable discussions at all stages of the project and for providing constructive comments on the manuscript.

Conflicts of interest

There are no conflicts to declare.

Notes and references

1 F. M. Akwi and P. Watts, *Chem. Commun.*, 2018, **54**, 13894–13928.
2 G. S. Fleming and A. B. Beeler, *J. Flow Chem.*, 2017, **7**, 124–128.
3 J.-I. Yoshida, Y. Takahashi and A. Nagaki, *Chem. Commun.*, 2013, **49**, 9896–9904.
4 B. Gutmann, D. Cantillo and C. O. Kappe, *Angew. Chem., Int. Ed.*, 2015, **23**, 6688–6728.
5 J. Britton and C. L. Raston, *Chem. Soc. Rev.*, 2017, **46**, 1250–1271.
6 J. Zhang, K. Wang, A. R. Teixeira, K. F. Jensen and G. Luo, *Annu. Rev. Chem. Biomol. Eng.*, 2017, **8**, 285–305.

Published on 28 May 2019. Downloaded by York University on 6/25/2019 5:11:38 PM.

7 M. B. Plutschack, B. Pieber, K. Gilmore and P. H. Seeberger, *Chem. Rev.*, 2017, **117**, 11796–11893.
8 J. G. Kralj, H. R. Sahoo and K. F. Jensen, *Lab Chip*, 2007, **7**, 256–263.
9 B. R. Fonslow and M. T. Bowser, *Anal. Chem.*, 2006, **78**, 8236–8244.
10 E. R. Castro and A. Manz, *J. Chromatogr. A*, 2015, **1382**, 66–85.
11 P. Novo and D. Janasek, *Anal. Chim. Acta*, 2017, **991**, 9–29.
12 N. W. Frost and M. T. Bowser, *Lab Chip*, 2010, **10**, 1231–1236.
13 P. L. Suryawanshi, S. P. Gumfekar, B. A. Bhanvase, S. H. Sonawane and M. S. Pimplapure, *Chem. Eng. Sci.*, 2018, **189**, 431–448.
14 F. J. Agostino, L. T. Cherney, V. Galievsky and S. N. Krylov, *Angew. Chem.*, 2013, **125**, 7397–7401.
15 A. C. Johnson and M. T. Bowser, *Lab Chip*, 2018, **18**, 27–40.
16 P. Novo, M. Dell'Aica, M. Jender, S. Höving, R. P. Zahedi and D. Janasek, *Analyst*, 2017, **142**, 4228–4239.
17 S.-I. Tobishima and A. Yamaji, *Electrochim. Acta*, 1984, **29**, 267–271.
18 J. Muzikar, T. van de Goor, B. Gaš and E. Kenndler, *Anal. Chem.*, 2002, **74**, 428–433.
19 F. J. Agostino, C. J. Evenhuis and S. N. Krylov, *J. Sep. Sci.*, 2011, **34**, 556–564.
20 S. Kochmann and S. N. Krylov, *Lab Chip*, 2017, **17**, 256–266.
21 R. Kuldvee, M. Vaher, M. Koel and M. Kaljurand, *Electrophoresis*, 2003, **25**, 1627–1634.
22 E. Kenndler, *J. Chromatogr. A*, 2014, **1335**, 16–30.
23 D. T. Walker, C. D. Douglas and B. J. MacLean, *Can. J. Chem.*, 2009, **87**, 729–737.
24 S. Kochmann and S. N. Krylov, *Anal. Chem.*, 2018, **90**, 9504–9509.
25 T. Okada, *J. Chromatogr. A*, 1997, **771**, 275–284.
26 S. P. Porras, R. Kuldvee, S. Palonen and M.-L. Riekkola, *J. Chromatogr. A*, 2003, **990**, 35–44.
27 V. Tandon, S. K. Bhagavatula, W. C. Nelson and B. J. Kirby, *Electrophoresis*, 2008, **29**, 1092–1101.
28 D. L. Pugmire, E. A. Waddell, R. Haasch, M. J. Tarlov and L. E. Locascio, *Anal. Chem.*, 2002, **74**, 871–878.
29 W. Schützner and E. Kenndler, *Anal. Chem.*, 1992, **64**, 1991–1995.
30 M. F. M. Tavares and V. L. McGuffin, *Anal. Chem.*, 1995, **67**, 3687–3696.
31 *Propylene carbonate*, MSDS No. O43314, Thermo Fisher Scientific, https://www.fishersci.com/store/msds?partNumber=O43314&vendorId=VN00033897&countryCode=CA (accessed Mar 08, 2019).
32 *Acetontrile*, MSDS No. A9981, Thermo Fisher Scientific, https://www.fishersci.ca/store/msds?partNumber=A9981&countryCode=CA&language=en (accessed Mar 08, 2019).
33 B. M. Rudisch, S. A. Pfeiffer, D. Geissler, E. Speckmeier, A. A. Robitzki, K. Zeitler and D. Belder, *Anal. Chem.*, 2019, **91**, 6689–6694.
34 B. R. Fonslow and M. T. Bowser, *Anal. Chem.*, 2005, **77**, 5706–5710.
35 M. Nissum and A. L. Foucher, *Expert Rev. Proteomics*, 2008, **5**, 571–587.
36 S. Köhler, C. Benz, H. Becker, E. Beckert, V. Beushausen and D. Belder, *RSC Adv.*, 2012, **2**, 520–525.
37 S. Köhler, S. Nagl, S. Fritzsche and D. Belder, *Lab Chip*, 2012, **12**, 458–463.
38 S. A. Pfeiffer, B. M. Rudisch, P. Glaeser, M. Spanka, F. Nitschke, A. A. Robitzki, C. Schneider, S. Nagl and D. Belder, *Anal. Bioanal. Chem.*, 2018, **410**, 853–862.

 This journal is © The Royal Society of Chemistry 2019

Electronic Supplementary Material (ESI) for Lab on a Chip.
This journal is © The Royal Society of Chemistry 2019

SUPPLEMENTARY INFORMATION

Non-Aqueous Continuous-Flow Electrophoresis (NACFE): Potential Separation Complement for Continuous-Flow Organic Synthesis

Nikita A. Ivanov, Yimo Liu, Sven Kochmann and Sergey N. Krylov

Centre for Research on Biomolecular Interactions and Department of Chemistry, York University, Toronto, Ontario M3J 1P3, Canada

Table of Contents

Additional supplementary files

These files can be found on ChemRxiv (https://doi.org/10.26434/chemrxiv.7840937):

File name	Description/Experiment
Angulagrams.zip	Extracted angulagrams and evaluation parameters for Figure 2, 3, and S4
Angulagrams10h.zip	Extracted angulagrams for the 10-h separation shown in Figure 4
Geometry.zip	Solid Edge files of chip geometry
Plots.zip	Origin files of all plots
Programs.zip	Python programs used to evaluate the data
Rawfiles.zip	Raw image files for Figure 2, 3, and S4
Rawfiles10h.zip	Raw image files for the 10-h separation shown in Figure 4
RawfilesCurrent.zip	Raw data of the current measurements show in Figure S2
Video10h.avi	Video of the 10-h separation
Videocurrent.avi	Video of the current measurements

Properties of tested plastic materials

Table S1. Evaluation parameters of tested plastic materials. PMMA is our reference material and choice for aqueous-based continuous-flow electrophoresis. FEP, PSu, and PVC Type I are suitable candidates for non-aqueous electrophoresis, in principle. However, PVC Type I is optically clear, has the best cost-efficiency, and, thus, was chosen in the present studies.

Name[a]	OC[b]	Millability[c]	PC[d]	Costs[e] ($/dm³)	Costs[f] ($/chip)	Relative costs[g]
ABS	not clear	✔	✘	20	3	1.0
CLPS	not clear	✔	✔	100	13	4.3
CPVC	not clear	✔	✔	55	7	2.3
FEP	**semi-clear**	✔	✔	**535**	**70**	**23.3**
HDPE	not clear	✔	✔	10	2	0.7
PCa	clear	✔	✘	20	3	1.0
PE	not clear	✘	✔	70	9	3.0
PEEK	not clear	✔	✔	655	86	28.7
PETG	clear	✔	✘	15	2	0.7
PMMA	**clear**	✔	✘	**25**	**3**	**1.0**
PP	semi-clear	✘	✔	15	2	0.7
PPS	not clear	✔	✔	755	99	33.0
PS	not clear	✔	✘	15	2	0.7
PSu	**semi-clear**	✔	✔	**185**	**24**	**8.0**
PTFE	not clear	✔	✔	170	22	7.3
PVC Type I	**clear**	✔	✔	**30**	**4**	**1.3**
PVDF	not clear	✔	✔	200	26	8.7
UHMW	not clear	✔	✔	15	2	0.7

[a]ABS = Acrylontrile butadiene styrene, CLPS = Cross-linked polystyrene (Rexolite), CPVC = Chemical-resistant polyvinyl chloride, FEP = Fluorinated ethylene propylene, HDPE = High-density polyethylene, PCa = Polycarbonate, PE = Polyester, PEEK = Polyether ether ketone, PETG = Polyethylene terephthalate glycol, PMMA = Poly(methyl methacrylate), PP = Polypropylene, PPS = Polyphenylene sulphide, PS = Polystyrene, PSu = Polysulfone, PTFE = Polytetrafluoroethylene (Teflon), PVC Type I = Polyvinyl chloride Type I, PVDF = Polyvinylidene fluoride, UHMW = Ultra-high-molecular-weight polyethylene.

[b]Optical clarity in visible spectrum (non-transparent).

[c]Ability to mill plastics using our established protocols for PMMA.[11] (✘ = material tends to melt and/or fringe more easily than PMMA).

[d]Compatibility with propylene carbonate (PC): plastic can withstand continuous exposure to PC for at least 48 h without any obvious swelling or disintegration.

[e]Cost is given in Canadian Dollars and based on McMaster-Carr's price list of February 2019. They are listed here for pure illustration and a rough comparison.

[f]About 0.132 dm³ are required for the assembly of one chip. Electrodes and flow connectors not included in price.

[g]Relative to PMMA.

NACFE chip

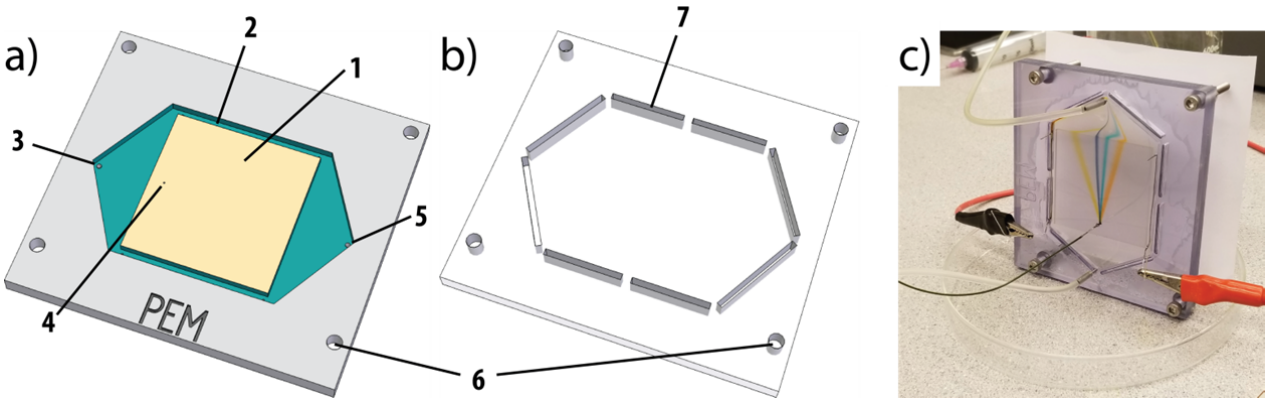

Figure S1. NACFE chip used in this study (named PEM after the city of Pembroke): **a)** bottom plate, **b)** top plate, and **c)** photo of assembled chip during operation. The numbers indicate: the separation zone (1), electrode channels (2), electrolyte inlet (3), sample inlet (4), outlet (5), mounting holes (6), and gluing channels (7). The chip dimensions are 110 mm × 100 mm × 12 mm, and the dimensions of the separation zone are 50 mm × 52 mm × 0.25 mm.

Electric current in NACFE with an electrolyte being TBAA solution in PC

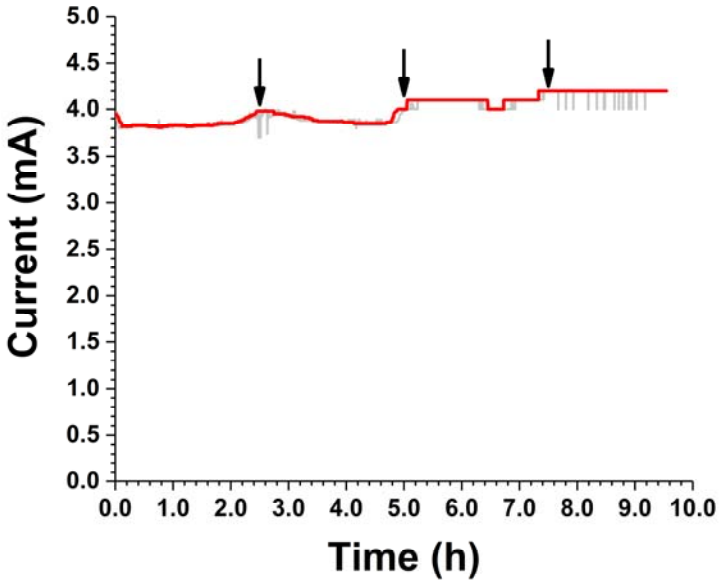

Figure S2. Long-term stability of NACFE using a solution of 30 mM TBAA in PC as an electrolyte. The arrows indicate the times at which the electrolyte was recycled. The grey curve is the signal as measured; the signal was smoothen for clarity by a percentile filter (100-point window; 80%); the red curve is the result of smoothening. The current was stable at 4.00 ± 0.15 mA (E = 18.2 V/cm) with only a slight drift towards higher currents due to electrochemical reactions and/or buffer depletion.

Formation of brown precipitate at the cathode for the imidazolium-based electrolyte

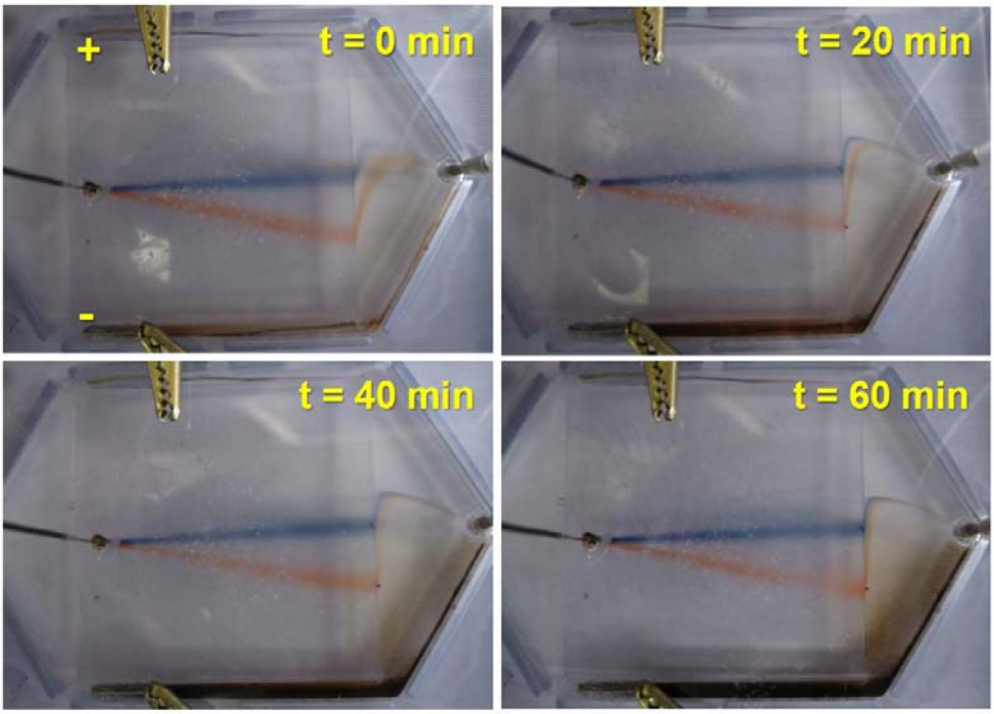

Figure S3. Separation of Sudan black B and Rhodamine 6G (3 mM each) in 21 mM imidazolium ethyl sulfate in PC. The excessive precipitation of a brown product at the cathode (bottom) affects optical clarity of the chip.

Comparing NACFE with weak- and strong-basicity anions in the electrolyte

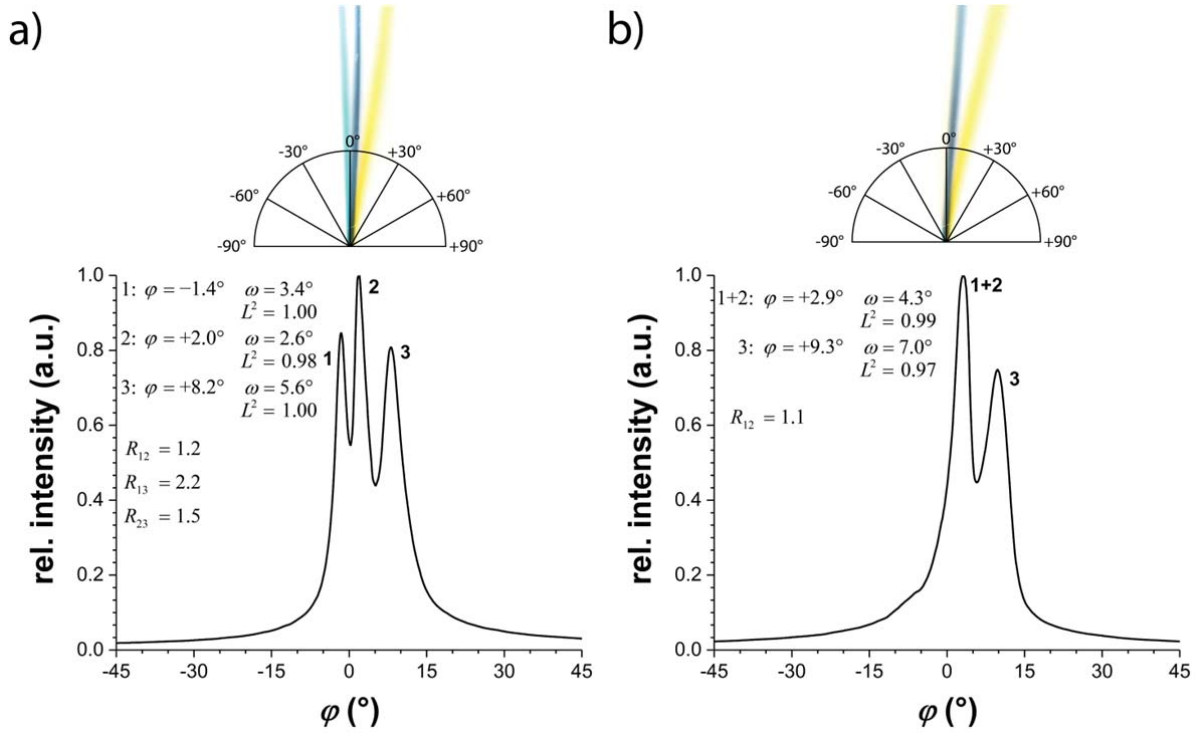

Figure S4. Separations with **a)** TBAA (strong base anion) and **b)** tetrabutylammonium hydrogen sulfate (weak base anion) in PC as electrolyte. Analytes were α-naphtholbenzein (1), Sudan black B (2), and DMAS (3). Only the strong-base anion was able to separate all three analytes. The conditions were: electrolyte flow rate = 3 mL/min, sample flow rate = 2 μL/min, and E = 27.3 V/cm ($I \approx 8.8$ mA). The anode and cathode are towards negative and positive angles, respectively.

Acetonitrile as solvent in non-aqueous electrolyte

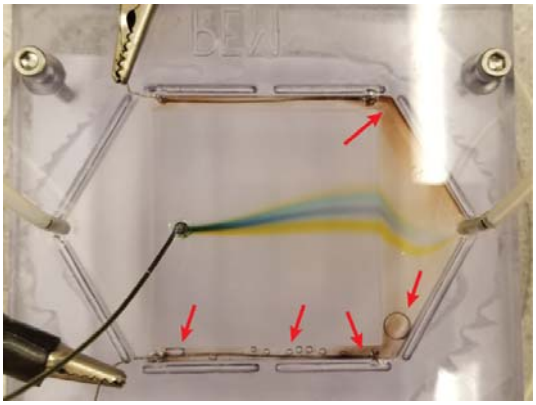

Figure S5. NACFE of four analytes (fluorescein, α-naphtholbenzein, Sudan black B, and DMAS; 1.25 mM each) in an electrolyte containing 30 mM TBAA in acetonitrile. Bubble formation (red arrows) and lack of bubble dislodging from the electrodes are evident. Bands are broader and higher electric fields are needed to achieve resolution similar to that in the PC-based electrolyte. Conditions were: electrolyte flow rate = 4 mL/min, sample flow rate = 2 μL/min, and E = 5.3 V/cm ($I \approx 8.0$ mA).

General handling procedures and experiences with NACFE

Materials and chemicals. All solutions were prepared using analytical grade reagents. Acetonitrile, α-naphtholbenzein, 2-[4-(dimethylamino)styryl]-1-methylpyridinium iodide, fluorescein sodium salt, imidazolium ethyl sulfate, PC, rhodamine 6G, Sudan black B, and TBAA were purchased from Sigma Aldrich (Oakville, ON, Canada). Electrolytes were solutions of imidazolium or tetrabutylammonium salts in PC or acetonitrile. Stock solutions of analytes were prepared in respective electrolytes as solvents. All chip materials listed in **Table S1** were purchased from McMaster Carr (Elmhurst, IL, USA).

Instrumentation. The electrolyte was delivered to the NAFCE chip with an NE-9000G peristaltic pump from New Era Pump Systems, Inc. (Farmingdale, NY, USA). The pump was equipped with a Masterflex pulse dampener from Cole Palmer (Vernon Hills, IL, USA) to suppress flow pulsation. Analyte solutions were delivered to the NACFE chip with a Model 11 syringe pump from Harvard Apparatus (Holliston, MA, USA). Separation voltage was applied to the platinum electrodes inside the separation zone from an EPS 3501 XL power supply from GE Healthcare (Chicago, IL, USA). NACFE chips were fabricated using a MODELA MDX-540 Benchtop Milling Machine from Roland DGA (Irvine, CA, USA).

Chip Fabrication. NACFE chips were designed in Solid Edge (see model files in **geometry.zip**) and fabricated of PVC Type I according to our previously developed fabrication procedure for PMMA chips (*J. Sep. Sci.* **2011**, *34*, 556−564, DOI: **10.1002/jssc.201000758**; *Lab Chip* **2017**, *17*, 256-266, DOI: **10.1039/C6LC01381C**). Details on chip fabrication and chip components used (apart from the chip material) may be found in these two previous works.

General experimental details. Electrolyte and analyte flow rates were in the ranges of 2−4 mL/min and 1−2 µL/min, respectively. 30−150 V were applied as separation voltages resulting in field strengths of 5−28 V/cm (distance between electrodes = 5.5 cm), respectively. Recycling for the 10-h separation was done in discrete steps transferring the electrolyte from the outlet container to the source container (feeding the peristaltic pump) roughly every 2.5 h.

Mixing behaviour of PC. PC and water are not miscible at similar ratios (*e.g.* 50:50). Therefore, water can be used to extract TBAA or other salts from the PC phase; aqueous workup of TBA-salts is a common technique (see *e.g.* DOI: 10.1021/ol063113h). The organic compounds will remain mainly in the PC phase (extraction coefficients can be further tuned by adding acid or base to water or by washing with diethyl ether):

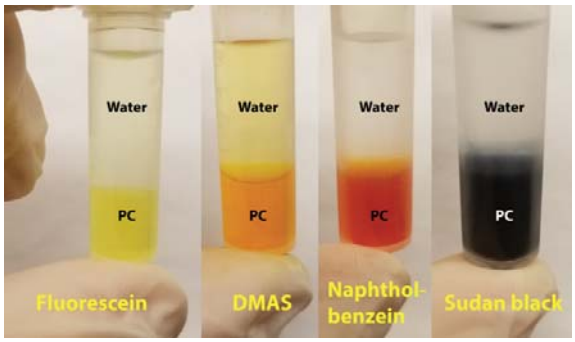

PC (boiling point at 1 atm ≈ 240 °C) can then be removed by rotary evaporation to yield the pure organic compounds. Note that at high concentrations of TBAA (1 M), water and PC phases become miscible and no phase separation can be observed. Similar, at low PC:water ratios (lower than 20:80, see DOI: 10.1021/je00028a012), PC and water mix and form a one-phase system. However, any organic compound previously dissolved in PC will precipitate; the precipitate can be further washed with cold water to remove remaining TBAA (and other salts). PC is also not miscible with hexane; therefore, hexane can be used to directly extract the organic compounds from PC if applicable (see *e.g.* DOI: 10.1021/cr900393d).

Evaluation procedures for NACFE images

The following procedures are mostly an implementation and extension of the concepts and programs in our previous work: *Anal. Chem.* **2018**, *90*, 9504−9509, DOI: **10.1021/acs.analchem.8b02186**. The basic idea is to represent molecular stream separation by a single plot, called angulagram. In an angulagram, every stream is represented by a single peak. Peak properties, such as position and shape, contain all information required to calculate quantitative stream characteristics: stream deflection, stream width, and stream linearity. The source code of all programs described here can be found in the Supplementary Files on Github (DOI: **10.5281/zenodo.2592588**) and ChemRxiv (DOI: **10.26434/chemrxiv.7840937**).

Constructing angulagrams from reflectometric images. The general procedure of angulagram construction is the same as the one used for fluorescence images in the previous work, namely i) aligning the image (rotation/mirroring), ii) cropping the region of interest (separation zone), iii) transferring the data from Cartesian to polar coordinates, and iv) integrating the signal over the radius. In contrast to fluorescence images, a reflectometric input image naturally includes a high background, which can be filtered out by lowering the color saturation and extracting only the hue levels of interest. The respective parameters were manually determined in Photoshop using the ruler tool (rotation angle, inlet position, and separation zone size) and adjustments tools (Image → Adjustments → Hue/saturation; Image → Adjustments → Levels); these parameters were then fed into a Python program (**angureflexin.py**) that performed the construction (see source code for details). The generated output consisted of an angulagram, a parameter file that listed all used parameters, an image of the separation zone in polar coordinates, and a preview image that was used as thumbnail for the angulagrams in this work.

Extracting stream parameters form angulagrams. Another Python script (**evolutin.py**) was used to find the stream peaks in the angulagrams and determine their parameters (deflection, width, linearity, and resolution) as described in our previous work. See the source code for details.

Evaluation of the 10-h separation. Angulagrams for all 3587 images (taken every 10 s) were created using batch processing by a Python script (**angulagrams10h.py**, processing time: 8.5 h) using the Python script (**angureflexin.py**) and the method described above. Parameters (rotation angle, color saturation, hue levels, etc.) were pre-determined for a set of 38 images across the whole separation (see **sampleparameters.csv**). They were found to be similar for these 38 images; therefore, their averages were used for the whole set of 3587 images. The resulting angulagrams were subsequently evaluated and stream parameters were extracted (**streameval10h.py** and **streampara10h.py**, processing times: about 45 min each) using the Python script (**evolutin.py**) and the method described above. Parameters needed for evaluation (background, window size for extrema finding, etc.) were pre-determined for a sample set. Before extracting stream parameters from the angulagrams, angulagrams were smoothened by a Savitzky-Golay filter (window size = 31, polynomial order = 3) to ensure the stability of the used numerical methods for finding minima/maxima etc. Finally, an integrated image based on all 3587 images was calculated (**integrate10h.py**) and presented in Figure 4d. A video files was generated by reducing the resolution of the images and encoding them with the XVID codec (**makevideo10h.py**).

Electrical current measurements. An EPS 3501 XL Electrophoresis Power Supply was used to set the electrophoresis voltage and measure the current. However, this device has no direct output (RS232 or the like) to sample the current data. Therefore, we used a camera to observe the display and then used an optical character recognition (OCR) approach to extract the current values. This was implemented as another Python script (**extract_currents.py**) using OpenCV (Open Source Computer Vision Library, https://opencv.org/) and Google's Tesseract engine (https://github.com/tesseract-ocr/tesseract). See source code for details. A video files was generated by reducing the resolution of the images and encoding them with the XVID codec (**makevideo10h.py**).